

NATIONAL AERONAUTICS AND SPACE ADMINISTRATION

LOAN COPY: RET  
AFWL TECHNICAL  
KIRTLAND AFB

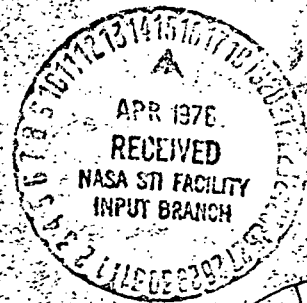


*Technical Memorandum 33-765*

*Improved Space Radiation  
Shielding Methods*

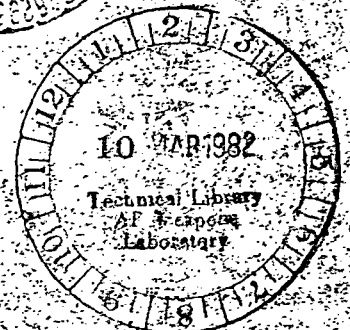
*Herbert S. Davis  
Thomas M. Jordan*

(NASA-CR-146581) IMPROVED SPACE RADIATION N76-21242  
SHIELDING METHODS (Jet Propulsion Lab.)  
34 p HC \$4.00 CSCL 22B  
G3/15 21504  
Unclas



JET PROPULSION LABORATORY  
CALIFORNIA INSTITUTE OF TECHNOLOGY  
PASADENA, CALIFORNIA

March 1, 1976





NATIONAL AERONAUTICS AND SPACE ADMINISTRATION

*Technical Memorandum 33-765*

*Improved Space Radiation  
Shielding Methods*

*Herbert S. Davis*

*Thomas M. Jordan*

JET PROPULSION LABORATORY  
CALIFORNIA INSTITUTE OF TECHNOLOGY  
PASADENA, CALIFORNIA

March 1, 1976

## PREFACE

The work described in this report was performed by the Applied Mechanics Division of the Jet Propulsion Laboratory under the cognizance of the Mariner Jupiter/Saturn 1977 Project. The work was originally prepared as a paper which was presented at the Winter Meeting of the American Nuclear Society held in San Francisco, California, on November 16-21, 1975.

## CONTENTS

I.	Introduction .....	1
II.	Summary .....	1
	A. Data Flow .....	1
	B. Software .....	2
III.	One-Dimensional Calculations .....	3
	A. Slant Path and Center-of-Sphere Kernels .....	3
	B. SHIELD Program .....	4
	C. Minimum Path and Angular Transmission Kernels .....	5
IV.	Complex Geometry Modeling .....	6
	A. Surface and Region Processors .....	6
	B. Electronics Bays Processors .....	7
	C. Boards Processor .....	7
	D. Design Processor .....	7
	E. Rotate and Translate Processors .....	7
	F. Camera and Picture Processors .....	8
V.	Three-Dimensional Calculations .....	8
	A. SIGMA Program .....	8
	B. Shield Optimization .....	9
VI.	Conclusions .....	10
	References .....	11
APPENDIXES		
	A. SHIELD, Numerical Method .....	19
	B. Minimum Path Kernel .....	28

PRECEDING PAGE BLANK NOT FILMED

## FIGURES

1.	Mariner Jupiter/Saturn 1977 spacecraft .....	12
2.	Electron and proton radiation transport software flow diagram .....	12
3.	BETA II/SHIELD/CHARGE comparison for spherical geometry .....	13
4.	SHIELD/BETA II/SIGMA comparison for slab geometry .....	13
5.	SHIELD/SANDYL comparison for transmission through a 2-cm slab of aluminum .....	14
6.	Schematic illustration of the sequence of rotations and translations used in SIGMA to position an electronics bay at its proper location in the spacecraft ..	15
7.	Computer plot of the command computer subsystem. The geometry model consists of 244 quadratic surfaces bounding 142 material regions .....	16
8.	Computer plot of the photopolarimeter subsystem. The geometry model consists of 108 quadratic surfaces bounding 56 material regions. ....	17
9.	Shield sensitivities for the Canopus tracker for one dose point . ....	18
10.	Shield weight optimization for the Canopus tracker for one dose point .....	18

---

## ABSTRACT

The computing software that was used to perform the charged particle radiation transport analysis and shielding design for the Mariner Jupiter/Saturn 1977 spacecraft is described. Electron fluences, energy spectra and dose rates obtained with this software are presented and compared with independent computer calculations.

## I. INTRODUCTION

In situ measurements of the Jovian trapped radiation were made by Pioneer 10 in December 1973 and by Pioneer 11 in December 1974. These measurements revealed a potentially hazardous environment for MJS'77 spacecraft electronics and some surfaces. As a result, the Mariner Jupiter/Saturn 1977 project carried out an intensive study of the charged particle environment derived from those measurements and the effects of that environment on both spacecraft and mission design (Ref. 1). This report covers one aspect of that study: the radiation transport analysis and shielding design.

Radiation analyses were performed for virtually all of the engineering and science subsystems of the MJS'77 spacecraft (Fig. 1) with the computer programs described in this report. System level and subsystem level shielding for the MJS'77 spacecraft were based on these radiation shielding calculations.

## II. SUMMARY

### A. DATA FLOW

A flow diagram of the main computer programs is shown in Fig. 2. Unshielded electron and proton radiation environments are input to the SHIELD program in the form of flux and fluence energy spectra for a particular trajectory derived from Jupiter electron and proton and solar flare proton radiation models (Ref. 1). The SHIELD program outputs include one-dimensional attenuation kernels such as dose or fluence vs absorber thickness for electrons, protons and secondary photons (bremsstrahlung).<sup>1</sup> This information, along with the spacecraft and/or subsystem geometry and mass distribution descriptions, is input to the SIGMA program (Ref. 2), which uses three-dimensional ray tracing to obtain dose and fluence estimates at internal spacecraft locations. The SOCODE program then uses the SIGMA shield sensitivity data in combination with a predetermined set of radiation level criteria to obtain an optimum shield configuration.

---

<sup>1</sup> Dose is generally expressed in units of rads, where a rad represents 100 ergs of energy deposited per gram of material. In this report the material is silicon.

## B. SOFTWARE

Several charged particle shielding codes were developed and/or revised during the course of this work. The SHIELD program, written at the Jet Propulsion Laboratory, subdivides materials into many small layers; within each layer, incident particles are transported using the continuous slowing down approximation for a set of solid angle bins. The angular distribution is revised at the surface of each layer using angular straggling distributions. The revised distribution is then used as the incident data for the next layer. SHIELD uses the BETA-II program (Ref. 3) cross section and source spectra processors. Output includes angular fluxes and flux responses with slab and center-of-sphere kernels, both printed and punched. Results for both differential and integral fluence are in excellent agreement with calculations performed using the BETA-II and SANDYL (Ref. 4) Monte Carlo computer programs.

The original SIGMA complex geometry program interpolated center-of-sphere kernels using slant path mass thicknesses for each ray used in the solid angle integration. This kernel agrees with Monte Carlo calculations for spherical geometry but underestimates radiation levels for slab geometry. A revised kernel was implemented which agrees with Monte Carlo calculations for both slab and spherical geometries. The revised kernel uses perpendicular mass thickness (estimated from slant paths and normal derivatives at material boundaries) in conjunction with a depth-dependent power law for angular transmission.

The geometry description and ray tracing portions of SIGMA received extensive modifications, including simple input for multiple bay spacecraft, recognition of simple geometric shapes with multiple bounding surfaces, and implementation of CRT plotting capabilities. In addition, the requirement for explicit description of void volumes was removed.

The shield sensitivity option of SIGMA was extended to include automatic recognition and retention of shield crossing combinations. This sensitivity information is used for designing spot shields for critical components and/or increasing vehicle surface thicknesses in an optimum manner.



### III. ONE-DIMENSIONAL CALCULATIONS

#### A. SLANT PATH AND CENTER-OF-SPHERE KERNELS

A typical one-dimensional attenuation kernel is the radiation level,  $D_{\text{sphere}}(x)$ , at the center of a sphere of radius  $x$ , due to an externally incident, cosine-distributed radiation source (isotropic flux environment). This is the kernel used by the original SIGMA program. The kernel can be generated by several methods and is supplied to the three-dimensional program as a tabulation of radiation level vs mass thickness.

The CHARGE program (Ref. 5) is a one-dimensional code which uses the basic range-energy relation, modified by applying electron transmission factors derived from curve fit Monte Carlo data (Mar formula, Ref. 6).

The BETA-II program uses Monte Carlo methods to predict electron transmission. Center-of-sphere results were approximated in slab geometry by

$$D_{\text{sphere}}(x) = \frac{4\pi}{\Delta\Omega} \Delta D(x, \cos \theta)$$

where  $x$  is the mass thickness of a slab,  $\theta$  is the off-normal scattering angle, and  $\Delta D(x, \cos \theta)$  is the radiation level contribution from the forward directed portion ( $0.9 < \cos \theta < 1.0$ ) of the electron transmission; i. e., only those particles transmitted within  $\Delta\Omega$  steradians of the slab normal are counted.

Figure 3 is a comparison of a one-dimensional kernel as generated for the Jupiter electron environment (Ref. 1) using the CHARGE and BETA-II programs. Both problems assume incident isotropic flux and cosine source angular dependence for an aluminum spherical shell absorber with the dose point at the center.

Excellent agreement between CHARGE and BETA-II was obtained through  $4 \text{ g/cm}^2$ . Divergence beyond  $4 \text{ g/cm}^2$  is attributed to the treatment, by CHARGE, of the high-energy ( $>10 \text{ MeV}$ ) content of the Jupiter electron environment. First, the Mar transmission formula was based on earth trapped radiation energies; i. e.,  $<10 \text{ MeV}$ . Second, CHARGE assumes that electrons slow down while traveling on straight lines (i. e., straight ahead

approximation). This assumption leads to overly conservative fluence estimates.

## B. SHIELD PROGRAM

The SHIELD program was written to retain the cost effectiveness of CHARGE kernel generation while removing the deficiencies for energies greater than 10 MeV. SHIELD uses the BETA-II electron/photon cross section processing; however, kernels are generated by numerically integrating the one-dimensional transport equation.

Numerical methods used in the SHIELD program include (see Appendix A):

- (1) Subdividing material layers into many differential sublayers.
- (2) Using condensed history angular straggling distributions (Goudsmit - Saunderson method) for each differential sublayer.
- (3) Regrouping of electrons after each differential sublayer into a fixed energy/angle mesh before proceeding to the next sublayer.

The efficacy of this approach, i. e., the excellent agreement with Monte Carlo calculations, is seen in Fig. 3. The BETA-II calculation used separate runs for the high (>10 MeV) and low (<10 MeV) energy portions of the spectrum. The SHIELD run required about one minute of Univac 1108 time, while the BETA-II calculation required over 30 min.

Other SHIELD capabilities include:

- (1) Energy-dependent flux output.
- (2) Angular flux output.
- (3) Multiple response functions.
- (4) Punched card output kernels for SIGMA.
- (5) Proton/heavy charged particle transport.
- (6) Secondary bremsstrahlung kernels.
- (7) Angular incidence, including monodirectional.

### C. MINIMUM PATH AND ANGULAR TRANSMISSION KERNELS

The major deficiency of slant path kernels is that they are correct only if material distributions around a receptor are actually spherically symmetric or if the charged particles are not deflected during transport.

Figure 4 indicates the error introduced by using slant path kernels with the Jupiter environment (Ref. 1) for simple uniform thickness slab geometry. In view of the unconservative results (underestimates) and of the many spacecraft volumes which have a slablike geometry (e. g., points just inside vehicle skins), an alternate one-dimensional kernel,  $D(x_{\min}(\mathbf{r}, \Omega))$ , was generated by SHIELD and implemented in SIGMA. In this kernel,  $x_{\min}(\mathbf{r}, \Omega)$  is the minimum mass thickness path at the dose point  $\mathbf{r}$  in the direction  $\Omega$ ; e. g., for slab geometry,  $x_{\min}(\mathbf{r}, \Omega)$  is the slab thickness, regardless of the relative direction between  $\Omega$  and the slab normal. This kernel is assumed to have an angular dependence of the form

$$D(z) = [D_{\text{sphere}}(z)] (\cos \phi)^{c(z)-1}$$

where  $z = x_{\min}(\mathbf{r}, \Omega)$ ,  $D_{\text{sphere}}(z)$  is the dose at the center of a spherical shell of thickness  $z$ ,  $\phi$  is the incident angle, and  $c(z)$  is a depth-dependent exponent. By requiring that this kernel correctly predict both center-of-sphere and slab geometry results,  $c(z)$  is simply

$$c(z) = \frac{D_{\text{sphere}}(z)}{D_{\text{slab}}(z)}$$

and is obtained directly from SHIELD calculations (see Appendix B). As seen in Fig. 4, this kernel is exact for slab geometries.

Using the SANDYL computer program, TRW reported (Ref. 7) additional verification of SHIELD-generated kernels. Typical differential fluence comparisons are shown in Fig. 5 for transmission through a 2 cm slab of aluminum.

#### IV. COMPLEX GEOMETRY MODELING

A description of the distribution of spacecraft materials (model) is required by SIGMA for radiation level calculations. The material distribution around specific dose points is obtained by ray tracing outward from these points.<sup>1</sup> The ray tracing methods of the FASTER III (Ref. 8)/BETA II/SIGMA programs required explicit descriptions of all volumes in a geometry, even if void. This requirement was removed because of lengthy input required to describe the many voids of complex shape in the spacecraft. The spacecraft models used in the kernel analysis are fully compatible with Monte Carlo analysis methods.

The SIGMA and BETA-II program files both utilize a series of user-oriented input/output data processors. The processors described below were used extensively.

##### A. SURFACE AND REGION PROCESSORS

Some parts of the spacecraft were described by the surface/region methods of the FASTER-III and BETA-II programs. Each region is defined by specifying the surfaces which form its boundaries, where each surface is defined by a general quadratic equation:

$$G(x, y, z) = a_0 + a_1x + a_2y + a_3z + a_4x^2 + a_5y^2 + a_6z^2 \\ + a_7xy + a_8yz + a_9zx = 0$$

where the  $a_k$  are the surface coefficients.

Material regions are then defined by specifying the particular surfaces (simple planes, cones, cylinders, or spheres) that bound that region. Regions of the MJS'77 spacecraft described by this method include the propellant tank and the high-gain antenna.

---

<sup>1</sup> Aluminum was used as the reference dose material.

The method of material distribution description given above was simplified for use by the MJS'77 project.

#### B. ELECTRONICS BAYS PROCESSORS

The MJS'77 spacecraft has ten electronics bays of similar geometry. An input processor was written to generate the surfaces and regions comprising each bay. Input parameters include:

- (1) Number of bays.
- (2) Thickness and materials of each bay wall.
- (3) Total weight and material of the bay interior.

In general, all bays except the one of specific interest were described by a smeared density which conserved mass, volume and shape.

#### C. BOARDS PROCESSOR

Several electronics bays had interiors containing a series of parallel electronics boards. An input processor was written to accept a simple input for parallel board geometries all having common transverse boundaries.

#### D. DESIGN PROCESSOR

Other electronics bays and all of the science instruments required more complicated geometric descriptions. They were composed of many parts, each with a different, but simple, geometry. Again, a special input processor was developed to generate the surfaces and regions required to describe these parts. Recognized shapes include plates, cylinders, annuli, spheres, and truncated cones. This processor included error testing for overlap of regions.

#### E. ROTATE AND TRANSLATE PROCESSORS

The interior of each bay was described in a bay-centered coordinate system. This description was then rotated and translated, by the program, to the appropriate spacecraft coordinates. This procedure is schematically indicated in Fig. 6.

This same rotation and translation capability was used for detector points; i. e., detectors were specified in the bay-centered coordinate system and then moved to the appropriate bay.

#### F. CAMERA AND PICTURE PROCESSORS

Two plotting routines were used to facilitate geometry checkout. One routine (PICTURE) generates printouts of geometry cross sections (Fig. 7). The second picture routine uses the CRT plot capabilities of the CAMERA program (Ref. 9 and Fig. 8).

### V. THREE-DIMENSIONAL CALCULATIONS

#### A. SIGMA PROGRAM

Radiation levels are calculated in the SIGMA program by numerical integration over solid angle of the one-dimensional attenuation kernels. For example, the dose  $D(\mathbf{r})$  is given by

$$D(\mathbf{r}) = \frac{1}{4\pi} \int_{4\pi} D(\mathbf{x}(\mathbf{r}, \Omega)) d\Omega = \frac{1}{4\pi} \sum_{i=1}^n K_i D_i(\mathbf{x}(\mathbf{r}, \Omega)) \Delta\Omega_i$$

where  $D(\mathbf{x}(\mathbf{r}, \Omega))$  is the dose that would be received at the dos. point if the mass thickness  $\mathbf{x}(\mathbf{r}, \Omega)$  of materials encountered in the differential solid angle  $d\Omega$  about the direction  $\Omega$  were spherically symmetric about  $\mathbf{r}$ . The constant  $K_i$  is associated with the numerical integration scheme (e. g.,  $K_i = 1$  for midpoint integration). Typically, for MJS'77, the polar and azimuthal angles were each segmented into 26 divisions, making an angular integration grid of  $26 \times 26 = 676$  solid angle sectors (ray traces). Geometry mockup capabilities available in ray tracing programs such as SIGMA permit very accurate representation of mass distributions. SIGMA accepts multiple radiation-type kernels (electron dose, proton fluence, etc.). Ray tracing about a detector point is performed only once; as each ray trace is performed, the contribution to every radiation type is obtained. In particular, all SIGMA runs output both slant path (center-of-sphere) and minimum path (slab) results.

SIGMA outputs include mass path distribution (both slant path and minimum path) and sensitivity of radiation levels with respect to shielding added to particular (user-specified) surfaces. This shield sensitivity output includes recognition of unique shield crossing combinations, e. g., none, one, or combinations of two or more, with corresponding output for the variation of the radiation level when these shield thickness are varied. Typical dose sensitivity data for one dose point is shown in Fig. 9.

## B. SHIELD OPTIMIZATION

SIGMA obtains shield-sensitivity data for one or more detector points and optionally saves the data on a permanent file. These data are then available for shield optimization calculations.

Optimization calculations can be performed for multiple dose points, shields, and criteria. The user specifies the criteria upper limits and how each criterion is formed from the individual radiation kernels calculated by SIGMA. For example,

$$\begin{aligned} \text{Dose criterion} &= (1) \times (\text{minimum path electron dose kernel}) \\ &+ (1) \times (\text{slant path proton dose kernel}) \\ &+ (0) \times (\text{all other kernels}). \end{aligned}$$

The user also specifies the geometry and minimum and maximum shield thickness at each candidate shield location. Candidate shields are those specified for the original SIGMA calculation plus a unit shield for each point detector. Unit shields, which are spherical shields centered at the dose point, are not obtained if the maximum unit shield thickness is specified as zero.

The optimum shield configuration is calculated by iteratively incrementing shield thickness until all criteria are met. On each iteration, the change in the  $j$ th radiation level is calculated separately for an increment of  $\Delta t_i$  in the  $i$ th shield; i. e.,

$$\Delta L_{ji} = L_j(t + \Delta t_i) - L_j(t)$$

is the change in the jth radiation level due to changing the thickness  $t = t_1, t_2, \dots, t_n$  by  $\Delta t_i$  in the ith shield only.

The corresponding change in the total shield weight is calculated as

$$\Delta W_i = W_i(t + \Delta t_i) - W_i(t)$$

using weight equations for slab, cylindrical, and/or spherical geometries, either isolated or nested.

A combined relative shield worth is calculated as

$$Q_i = \frac{\sum_j (\Delta L_{ji} / L_j^0)}{\Delta W_i}$$

where the summation is over different radiation level criteria and  $L_j^0$  is the jth criterion. That shield for which  $Q_i$  is most negative is changed by a thickness  $\Delta t_i$  and the process is repeated until all criteria are met.

The results obtained for a single detector point and a single criterion are shown in Fig. 10. Because the optimization uses interpolations of tabulated sensitivity data, a SIGMA calculation for the optimized shield configuration agrees with the optimization output to within a few percent.

## VI. CONCLUSIONS

Ray tracing (sectoring) transport programs like SIGMA do have their limitations. The errors introduced by using one-dimensional attenuation kernels and by assuming that electrons do not scatter from one solid angle sector to another may be significant. Unfortunately, no experimental measurements that can be used for direct quantitative assessment of the accuracy of these programs have been made for three-dimensional shield configurations. Nevertheless, compared to Monte Carlo programs, the computer programs described in this report are fast, convenient, versatile, and inexpensive. Together, they represent a necessary capability for any project where space radiation shielding engineering is an essential discipline.



## REFERENCES

1. Mariner Jupiter/Saturn 1977 Radiation Control Requirements Document, PD 613-229, Revision A, Jet Propulsion Laboratory, Pasadena, Calif., Dec. 19, 1975 (an internal document).
2. Jordan, T. M., SIGMA, A Computer Program for Space Radiation Dose Analysis Within Complex Configurations, Report DAC-60878, McDonnell Douglas Corp., Huntington Beach, Calif., Nov. 1967.
3. Jordan, T. M., BETA-II, A Time-Dependent, Generalized-Geometry Monte Carlo Program for Bremsstrahlung and Electron Transport Analysis, ART-60, ART Research Corp., Los Angeles, Calif., Oct. 1971.
4. Colbert, H. M., SANDYL: A Computer Program for Calculating Combined Photon-Electron Transport in Complex Systems, Document SLL-74-0012, Sandia Laboratories, Livermore, Calif., Sept. 1974.
5. Yucker, W. R., and Lilley, J. R., CHARGE Code for Space Radiation Shielding Analysis, Report DAC-62231, McDonnell Douglas Corp., Huntington Beach, Calif., Apr. 1969.
6. Mar, B. W., "An Electron Shielding Analysis for Space Vehicles," Nuc. Sci. Eng., 24, 193, 1966.
7. Faelton, E. M., Robertson, L. D., and Gordon, J. D., Comparison and Reconciliation of TRW/JPL Dose and Equivalent Damage Fluence Calculations for the Flight Data Subsystem of the MJS'77 Spacecraft, Document 27679-6002-RU-00, TRW, Redondo Beach, Calif., May 30, 1975.
8. "FASTER-III, A Time Dependent, Generalized Geometry Monte Carlo Program for the Transport of Neutrons and Photons," ART-57, ART Research Corp., Los Angeles, Calif., July 1970.
9. M. P. Billings and W. R. Yucker, "The Computerized Anatomical Man (CAM) Model," Summary Final Report, MDC G4655, McDonnell Douglas Corp., Huntington Beach, Calif., Sept. 1973.

REPRODUCIBILITY OF THE ORIGINAL PAGE IS POOR

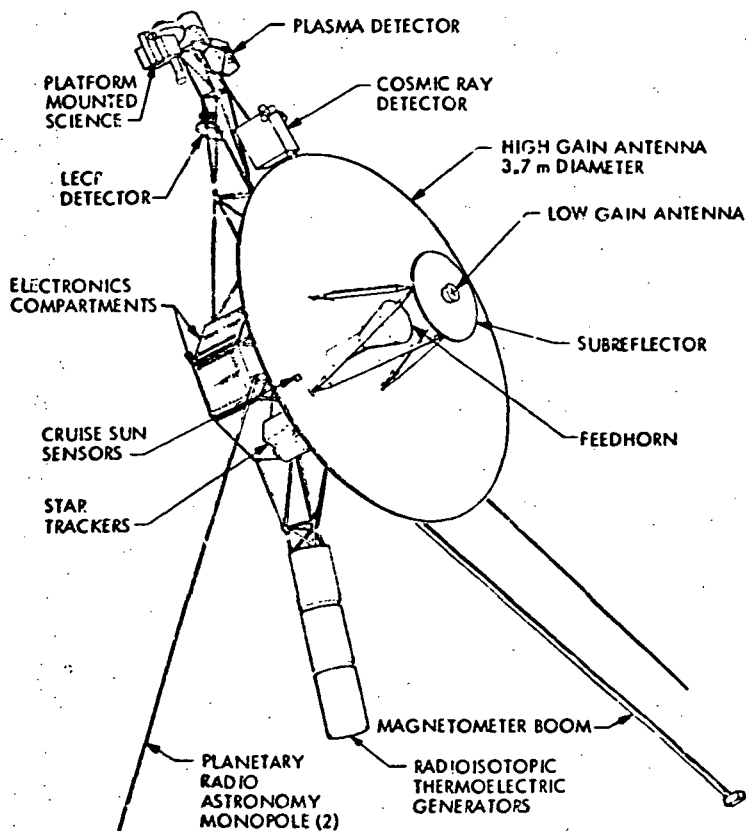


Fig. 1. Mariner Jupiter/Saturn 1977 spacecraft.

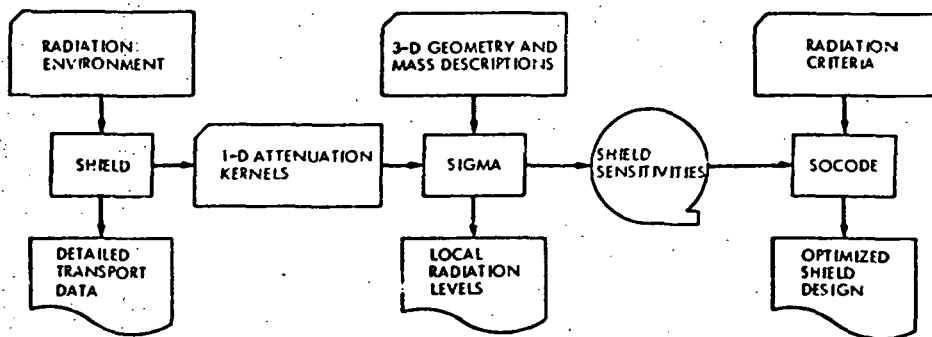


Fig. 2. Electron and proton radiation transport software flow diagram.

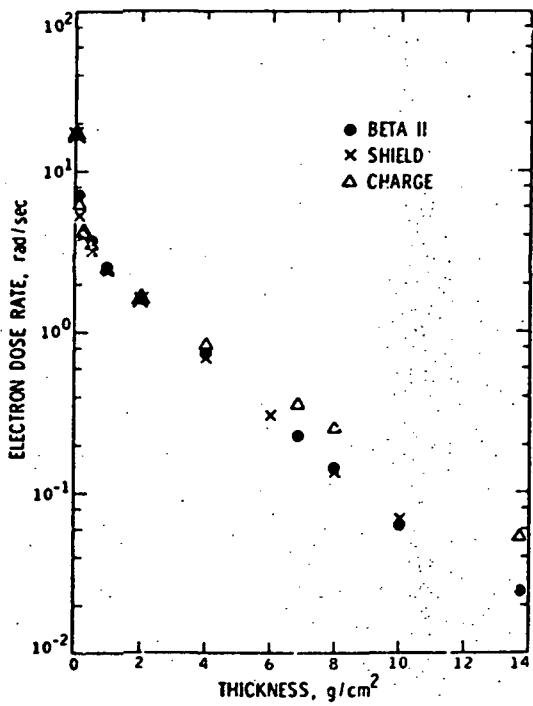


Fig. 3. BETA II/SHIELD/CHARGE comparison for spherical geometry.

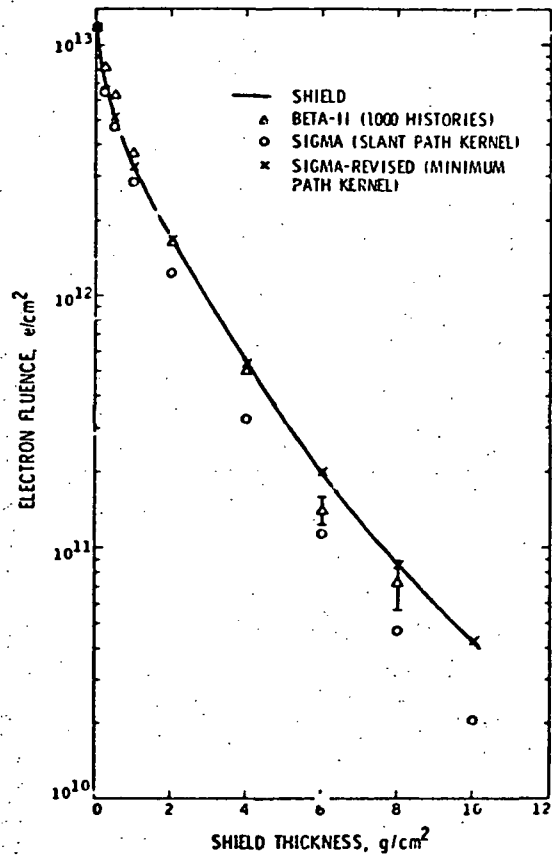


Fig. 4. SHIELD/BETA II/SIGMA comparison for slab geometry.

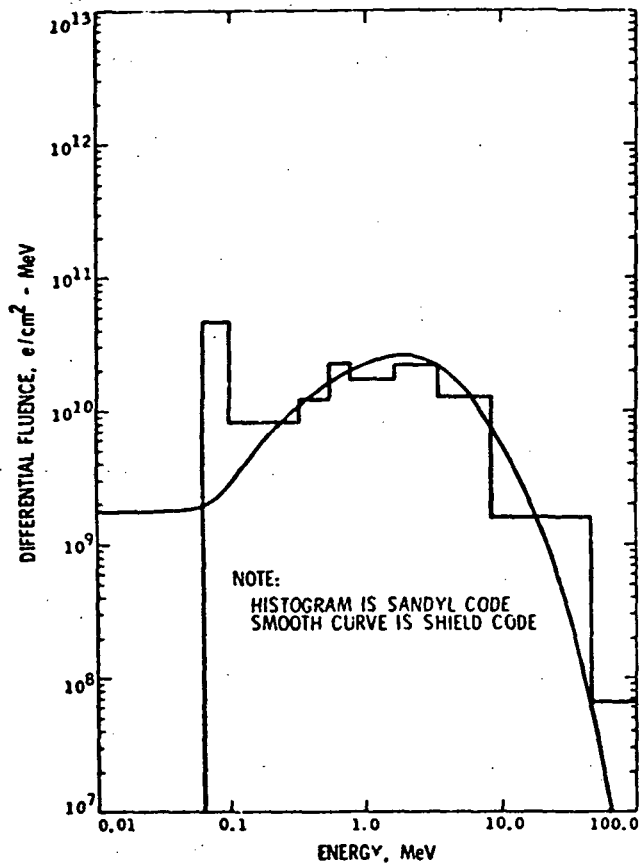


Fig. 5. SHIELD/SANDYL comparison for transmission through a 2-cm slab of aluminum.

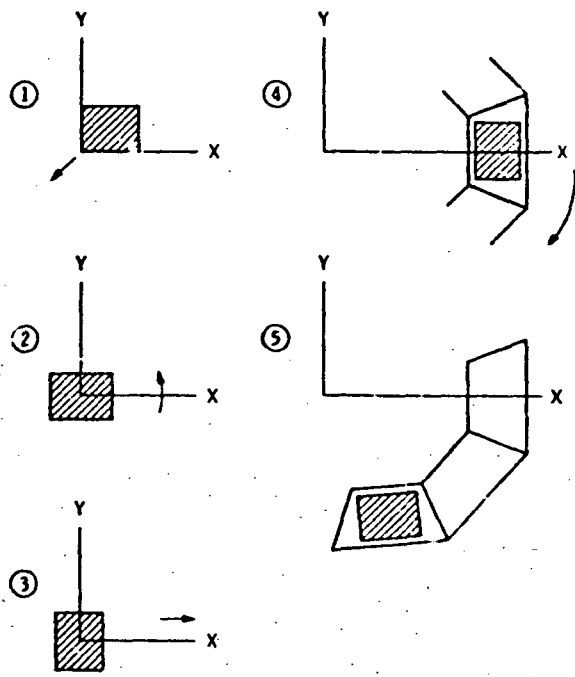


Fig. 6. Schematic illustration of the sequence of rotations and translations used in SIGMA to position an electronics bay at its proper location in the spacecraft.

REPRODUCIBILITY OF THE ORIGINAL PAGE IS POOR

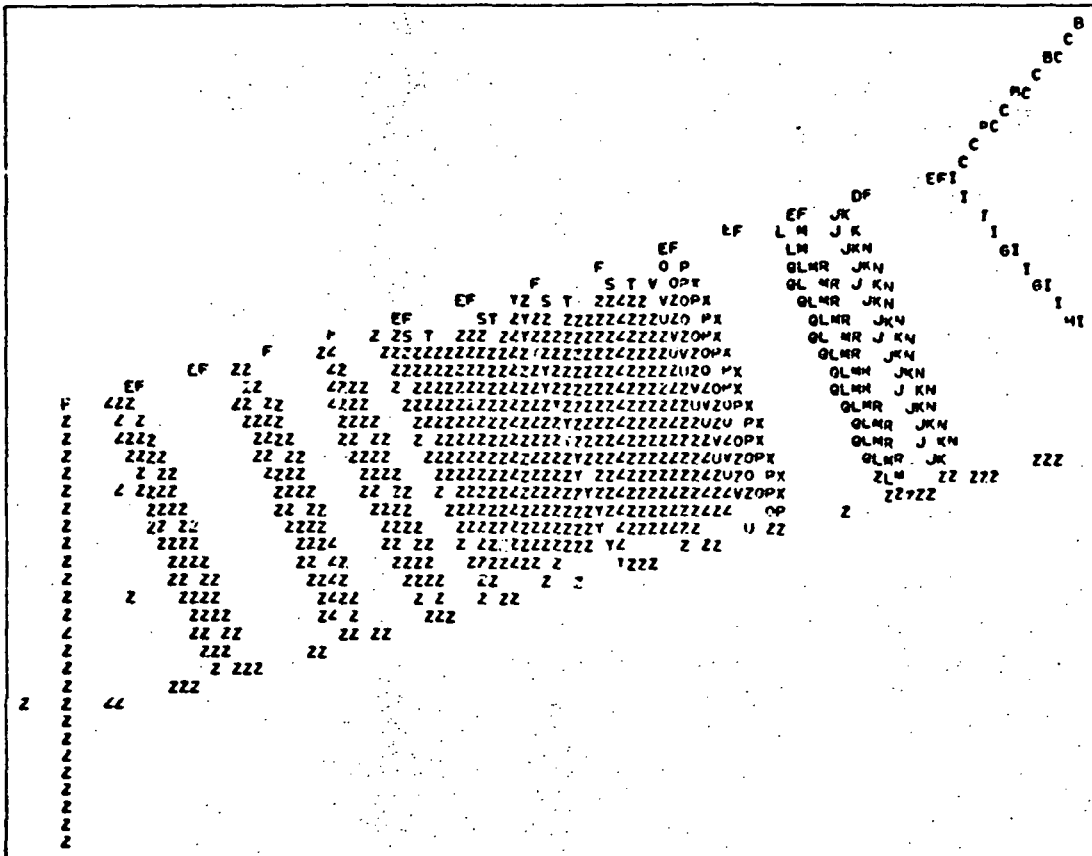


Fig. 7. Computer plot of the command computer subsystem. The geometry model consists of 244 quadratic surfaces bounding 142 material regions.

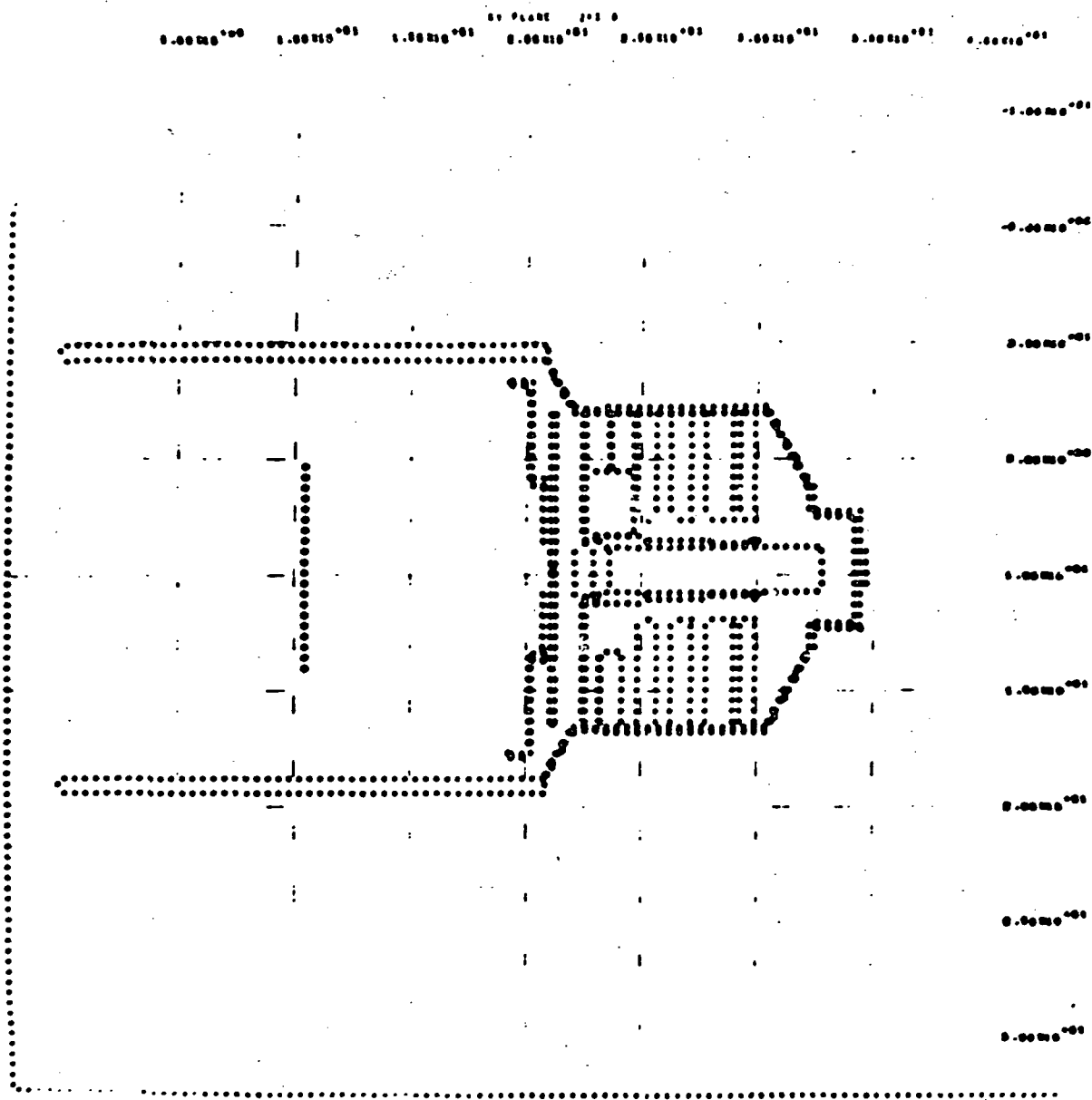


Fig. 8. Computer plot of the photopolarimeter subsystem. The geometry model consists of 108 quadratic surfaces bounding 56 material regions.

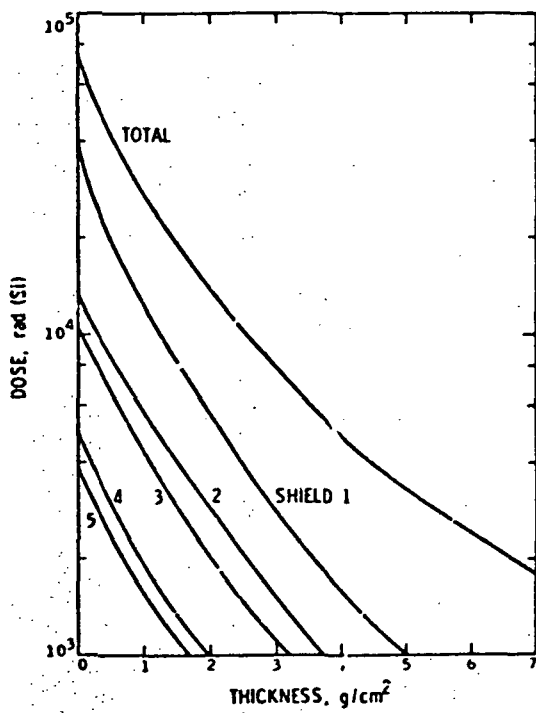


Fig. 9. Shield sensitivities for the Canopus tracker for one dose point.

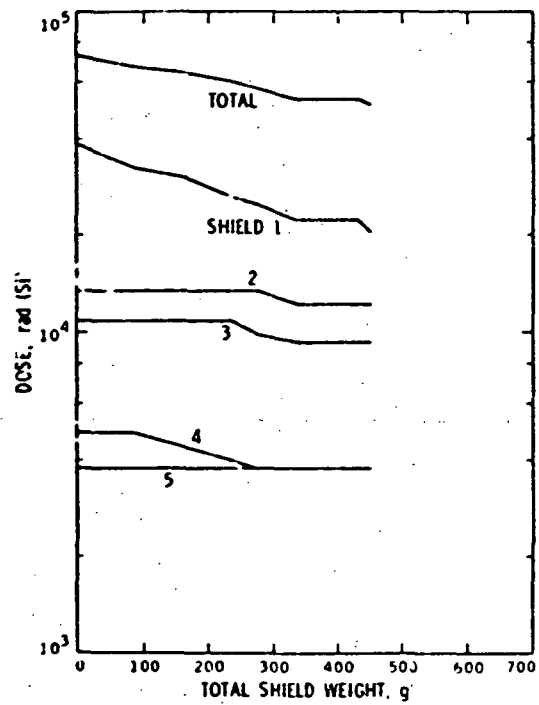


Fig. 10. Shield weight optimization for the Canopus tracker for one dose point.



APPENDIX A  
SHIELD, NUMERICAL METHOD

The SHIELD code calculates charged particle transport in one-dimensional geometries. The following definitions are used in the numerical integration.

I. DIRECTION VECTORS

Let  $\Omega$  denote the original particle direction

$$\Omega = (i \cos \theta + j \sin \theta) \sqrt{1 - \mu^2} + k\mu \quad \begin{cases} \theta = \text{azimuth} \\ \mu = \text{polar angle cosine} \end{cases} \quad (\text{A-1})$$

and  $\Omega'$  the deflected direction

$$\Omega' = (i \cos \theta' + j \sin \theta') \sqrt{1 - \mu'^2} + k\mu' \quad \begin{cases} \theta' = \text{azimuth} \\ \mu' = \text{polar angle cosine} \end{cases} \quad (\text{A-2})$$

Then the cosine of the deflection analysis

$$\mu_s = \Omega \cdot \Omega' = \sqrt{1 - \mu^2} \sqrt{1 - \mu'^2} \cos \omega + \mu\mu', \quad \omega = \theta' - \theta \quad (\text{A-3})$$

II. LEGENDRE POLYNOMIALS

By definition

$$P_0(\mu) = 1, \quad P_1(\mu) = \mu \quad (\text{A-4})$$

$$P_\ell(\mu) = \frac{1}{\ell} \left[ (2\ell - 1) P_{\ell-1}(\mu) - (\ell - 1) P_{\ell-2}(\mu) \right] \quad (\text{A-5})$$

$$P_\ell(\mu) = \frac{1}{2\ell + 1} \left[ \frac{dP_{\ell+1}(\mu)}{d\mu} - \frac{dP_{\ell-1}(\mu)}{d\mu} \right] \quad (\text{A-6})$$

$$\int_a^b P_\ell(\mu) d\mu = \frac{1}{2\ell+1} \left[ P_{\ell+1}(\mu) - P_{\ell-1}(\mu) \right]_a^b \quad (A-7)$$

The addition formula for azimuthal symmetry is equivalent to

$$P_\ell(\Omega \cdot \Omega') = P_\ell(\mu_s) = P_\ell(\mu) P_\ell(\mu') \quad (A-8)$$

For forward directions, the following is defined:

$$1 - P_\ell(\mu) = B_\ell(\mu) (1 - \mu) \quad (A-9)$$

It follows that

$$B_0(\mu) = 0, \quad B_1(\mu) = 1 \quad (A-10)$$

and from (A-9) and (A-5),

$$B_\ell(\mu) = \frac{1}{\ell} \left\{ (2\ell - 1) \left[ 1 + \mu B_{\ell-1}(\mu) \right] - (\ell - 1) B_{\ell-2}(\mu) \right\} \quad (A-11)$$

It can be shown by induction, using (A-11), that

$$B_\ell(\mu = 1) = \frac{\ell(\ell + 1)}{2} \quad (A-12)$$

Therefore,

$$\lim_{\mu \rightarrow 1} \left[ 1 - P_\ell(\mu) \right] = \frac{\ell(\ell + 1)}{2} (1 - \mu) \quad (A-13)$$

The expansion of a general function  $f(\mu)$  uses the coefficients  $f_\ell$ , where

$$f_\ell = 2\pi \int_{-1}^1 f(\mu) P_\ell(\mu) d\mu \quad (A-14)$$

i. e.

$$f(\mu) = \sum_{\ell=0}^{\infty} \frac{2\ell+1}{4\pi} f_{\ell} P_{\ell}(\mu) \quad (\text{A-15})$$

Finally, if for any function  $g(\mu)$

$$g(\mu) = g \frac{\delta(\mu-1)}{2\pi} \text{ (a delta function), then } g_{\ell} = g \text{ for all } \ell \quad (\text{A-16})$$

### III. SCATTERING CROSS SECTION

The charged particle deflection cross section has the form

$$\frac{d\sigma}{d\Omega}(\mu) = \frac{C}{(1-\mu+\eta)^2} \quad (\text{A-17})$$

where  $\eta$  is the screening angle, and  $\eta \ll 1 \Rightarrow$  strong peaking at  $\mu = 1$ .

It follows that

$$\sigma = 2\pi \int_{-1}^1 \frac{d\sigma}{d\Omega}(\mu) d\mu \quad (\text{A-18})$$

is the total cross section and the Legendre expansion coefficients are

$$\sigma_{\ell} = 2\pi \int_{-1}^1 \frac{d\sigma}{d\Omega}(\mu) P_{\ell}(\mu) d\mu \quad (\text{A-19})$$

in particular  $\sigma_0 = \sigma$ . Thus, the scattering cross section can be represented by

$$\frac{d\sigma}{d\Omega} = \sum_{\ell=0}^{\infty} \frac{2\ell+1}{4\pi} \sigma_{\ell} P_{\ell}(\mu) \quad (\text{A-20})$$

By definition (for later use),

$$\sigma_{\ell}^* = \sigma - \sigma_{\ell} = 2\pi \int_{-1}^1 \frac{d\sigma}{d\Omega}(\mu) [1 - P_{\ell}(\mu)] d\mu \quad (\text{A-21})$$

or equivalently,

$$\sigma_{\ell}^* = 2\pi \int_{-1}^1 \frac{d\sigma}{d\Omega}(\mu) B_{\ell}(\mu) (1 - \mu) d\mu \quad (\text{A-22})$$

With strong forward peaking, most of the integral comes from  $\mu \approx 1$ , so that

$$\sigma_{\ell}^* \approx 2\pi B_{\ell}(\mu=1) \int_{-1}^1 \frac{d\sigma}{d\Omega}(\mu) (1 - \mu) d\mu \quad (\text{A-23})$$

or

$$\sigma_{\ell}^* \approx \frac{\ell(\ell+1)}{2} b \quad (\text{A-24})$$

where

$$b = 2\pi \int_{-1}^1 \frac{d\sigma}{d\Omega}(\mu) (1 - \mu) d\mu \quad (\text{A-25})$$

Equality in Eq. (A-24) is used for  $\sigma_{\ell}^*$  rather than the exact value from Eq. (A-21) or (A-22).

#### IV. TRANSPORT EQUATION

The transport equation is written as a function of particle distance traversed, where

$$\phi(s, \mu) = \text{the angular flux at distance } s \quad (\text{A-26})$$

The Legendre moments of the flux are

$$\phi_m(s) = 2\pi \int_{-1}^1 \phi(s, \mu) P_m(\mu) d\mu \quad (\text{A-27})$$

Therefore, the angular flux can be represented by

$$\phi(s, \mu) = \sum_{m=0}^{\infty} \frac{2m+1}{4\pi} \phi_m(s) P_m(\mu) \quad (\text{A-28})$$

The transport equation, allowing only deflection reactions, is

$$\frac{\partial \phi}{\partial s}(s, \mu) = \int_{4\pi} \phi(s, \mu') \frac{d\sigma}{d\Omega}(s, \Omega' \cdot \Omega) d\Omega' - \sigma(s) \phi(s, \mu) \quad (\text{A-29})$$

Substituting for the scattering cross section yields

$$\begin{aligned} \frac{\partial \phi}{\partial s}(s, \mu) &= \int_{4\pi} \phi(s, \mu') \left[ \sum_{\ell=0}^{\infty} \frac{2\ell+1}{4\pi} \sigma_{\ell}(s) P_{\ell}(\mu) P_{\ell}(\mu') \right] d\mu' d\theta' \\ &\quad - \sigma(s) \phi(s, \mu) \end{aligned} \quad (\text{A-30})$$

$$= \sum_{\ell=0}^{\infty} \frac{2\ell+1}{4\pi} \sigma_{\ell}(s) P_{\ell}(\mu) \phi_{\ell}(s) - \sigma(s) \phi(s, \mu) \quad (\text{A-31})$$

Multiplying by  $P_m(\mu)$ , integrating over  $4\pi$ , and using

$$\int_{-1}^1 P_\ell(\mu) P_m(\mu) d\mu = \frac{\delta_{\ell m}}{2m+1} \quad (\text{A-32})$$

yields

$$\frac{\partial \phi_m}{\partial s}(s) = \sigma_m(s) \phi_m(s) - \sigma(s) \phi_m(s) = -[\sigma(s) - \sigma_m(s)] \phi_m(s) \quad (\text{A-33})$$

or, using the definition of  $\sigma_m^*$ ,

$$\frac{\partial \phi_m}{\partial s}(s) = -\sigma_m^*(s) \phi_m(s) \Rightarrow \frac{\partial}{\partial s} \ln \phi_m(s) = -\sigma_m^*(s) \quad (\text{A-34})$$

A simple integral yields the solution

$$\phi_m(s) = \phi_m(0) \exp \left[ - \int_0^s \sigma_m^*(s') ds' \right] \quad (\text{A-35})$$

where the  $\phi_m(0)$  are the Legendre moments at  $s = 0$ . Thus

$$\phi_m(0) = 2\pi \int_{-1}^1 \phi(0, \mu) P_m(\mu) d\mu \quad (\text{A-36})$$

Equations (A-35) and (A-36), and Eq. (A-21) for  $\sigma^*$ , constitute the Gaudsmit-Saunders method. The series is truncated at order  $L$  and a delta function component is assumed. Therefore,

$$\phi(s, \mu) = \tilde{\phi}(s, \mu) + \phi_L(s) \frac{\delta(\mu - 1)}{2\pi} \quad (\text{A-37})$$

The moments of this equation are

$$\phi_m(s) = \tilde{\phi}_m(s) + \phi_L(s) \quad (\text{A-38})$$

Therefore,

$$\tilde{\phi}_m(s) = \phi_m(s) - \phi_L(s) \quad (\text{A-39})$$

and

$$\phi(s, \mu) = \sum_{m=0}^{L-1} \frac{2m+1}{4\pi} [\phi_m(s) - \phi_L(s)] P_2^m(\mu) + \phi_L(s) \frac{\delta(\mu-1)}{2\pi} \quad (\text{A-40})$$

## V. TRANSPORT THROUGH MATERIALS

The above definitions are used for the charged particle transport in the following numerical scheme. First, the shield material thickness is divided into many small layers; each layer thickness is much less than the range of the lowest energy electrons. Second, the range of polar angle cosine relative to the layer normal is divided into many intervals; i. e., interval  $i$  is  $\mu_i \leq \mu \leq \mu_{i+1}$  where the  $\mu_i$ 's are the interval boundaries. The transport problem is then solved by repetitively calculating the transmitted energy-angle distribution for a layer and using that distribution as the incident source for the next layer.

In particular, let  $W_{ji}$  denote the number of incident particles in energy group  $j$  and angle interval  $i$ . Let  $E_{ji}$  denote the average energy of the particles. The problem is a calculation of  $W'_{ji}$  and  $E'_{ji}$  on the other side of a layer of thickness  $t$ ; i. e., for each energy group and angle interval,

$$\bar{\mu}_i = \frac{1}{2} (\mu_i + \mu_{i+1}), \text{ the average polar angle cosine}$$

$$s_i = \frac{t}{\bar{\mu}_i}, \text{ the path length across the layer}$$

$$E_{ji}'' = E_{ji} - \int_0^{s_i} \left| \frac{dE}{ds}(s') \right| ds' , \text{ the transmitted energy}$$

$$B_{ji} = \int_0^{s_i} b_j(s') ds' , \quad b(s) \text{ from (A-25)}$$

$$\phi_{ji}^0 = \exp \left[ -L(L+1) \frac{B_{ji}}{2} \right] , \text{ the fraction of particles transmitted into the same angle interval.}$$

The energy-angle distribution of deflected particles is

$$W_{ji}''(E', \mu', \theta') = W_{ji} \left[ \sum_{l=0}^{L-1} \frac{2m+1}{4\pi} A_{jim} \frac{P_m(\mu)}{2\pi(\mu_{i+1} - \mu_i)} P_m(\mu') \right] \delta(E' - E_{ji}'')$$

where

$$A_{jim} = \exp \left[ -m(m+1) \frac{B_{ji}}{2} \right] - \exp \left[ -L(L+1) \frac{B_{ji}}{2} \right] .$$

Integrating over the initial and final directions and adding on the undeflected component yields the energy distribution of transmission into angle interval  $i'$ :

$$W_{i'ji}''(E') = W_{ji} \left( \sum_{m=0}^{L-1} \frac{2m+1}{2} A_{jim} \frac{C_{im} C_{i'm}}{\mu_{i+1} - \mu_i} + \phi_{ji}^0 \delta_{i'i} \right) \delta(E' - E_{ji}'')$$

where  $C_{im}$  is the integral of the  $m$ th Legendre polynomial over the  $i$ th angle interval. Integration over final energy yields

$$W_{j'i'}' = \sum_i \sum_j \int_{\text{group } j'} W_{i'ji}''(E') dE'$$



and

$$E_{j'i'} = \frac{1}{W_{j'i'}} \sum_i \sum_j \int_{\text{group } j'} W_{i'ji}''(E') E' dE'$$

APPENDIX B  
MINIMUM PATH KERNEL

For isotropic incidence on both sides of a slab,

$$\begin{aligned}
 D(z) &= \left(\frac{1}{4\pi}\right)^2 \int_0^{2\pi} \int_{\cos \phi=0}^{\cos \phi=1} [D_{\text{sphere}}(z)] (\cos \phi)^{c(z)-1} d(\cos \phi) d\theta \quad (\text{B-1}) \\
 &= \int_0^1 D_{\text{sphere}}(z) \mu^{c(z)-1} d\mu, \quad \mu \equiv \cos \phi \\
 &= D_{\text{sphere}}(z) \left[ \frac{\mu^{c(z)}}{c(z)} \right]_0^1 \\
 &= \frac{D_{\text{sphere}}(z)}{c(z)} = \frac{D_{\text{sphere}}(z)}{\left( \frac{D_{\text{sphere}}(z)}{D_{\text{slab}}(z)} \right)}
 \end{aligned}$$

$$D(z) = D_{\text{slab}}(z)$$

For isotropic incidence on a sphere,  $\mu = 1$  and

$$D(z) = \frac{1}{4\pi} \int_0^{2\pi} \int_{\cos \phi=0}^{\cos \phi=1} [D_{\text{sphere}}(z)] (\mu)^{c(z)-1} d(\cos \phi) d\theta$$

so that, from (B-1)

$$D(z) = D_{\text{sphere}}(z)$$

**END  
DATE  
FILMED**

**JUN 7 1976**

**SHIPPED FROM NTIS**

**MAR 02 1982**